Theory of average charge and energy loss of cluster ions in foils

Toshiaki Kaneko
Department of Applied Physics, Okayama University of Science, 1-1 Ridai-cho, Okayama 700 0005, Japan
(Received 10 June 2002; published 20 November 2002)

We study the average charge and the electronic energy loss of the swift (but not relativistic) clusters in a solid. A self-consistent average-charge theory for clusters in foils is presented on the basis of the fluid-mechanical model. Here the electron stripping rate is evaluated not only for an isolated ion, but also for cluster ions under the same background by taking into account the binding effect of the surrounding ions. This theory can elucidate very well not only the reduction of the cluster average charge per ion, but also its cluster-size and foil-thickness dependences of the recent data for the MeV/atom carbon clusters (C_n) in carbon foils. The structure dependence is also proposed theoretically. In spite of the average-charge reduction, we can reconcile the enhancement of the energy losses of the corresponding clusters. The cluster energy losses with the inclusion of the Coulomb explosion by the wave-packet model is in much better agreement with the data at energies of 1–5.65 MeV/atom. Consistent agreement both in the diminution of average charge and in the enhancement of energy loss supports that the charge-state bulk effect is dominant in the cluster average charge.

DOI: 10.1103/PhysRevA.66.052901 PACS number(s): 34.50.Bw, 36.40.−c, 61.85.+p

I. INTRODUCTION

Since ion accelerators were widely applied to ion-material interaction, the charge-state distribution (CSD) of energetic ions emerging from a material has been one of central problems, especially at intermediate velocities where the bound electrons are partially stripped off. The reason for it is why charge states directly determine the coupling strength of the electromagnetic force in ion-material interactions. For heavy ions, as many charge states would incorporate, the experimental CSD data have been semiempirically analyzed by using statistical models, e.g., a Gaussian distribution [1] and a χ^2 distribution [2]. The first moment of the CSD, which is called the average charge, is often a more typical parameter than the CSD itself. For example, the Z_1 (projectile's atomic number) [3] and the Z_2 (target's atomic number) oscillations of the average charge were reported [4], which reflects the electronic shell structures. Such oscillations were also observed for the light-ion incidence [5]. From a microscopic point of view, the CSD is governed by the electron-capture and -loss processes. According to a theoretical study [6], the appearance of this oscillatory structure is due to the oscillatory behavior of the quasiresonance electron-capture cross section. It is well known that the average charge of an ion will attain to the equilibrium state after the ion penetrates a sufficiently thick target, as the memory of the initial charge state was completely lost. In the intermediate-energy region (more than a few keV/u but nonrelativistic), the equilibrium average charge depends mainly on the ion velocity, not so strongly dependent of the target materials. Even if a small oscillation would exist, the overall average-charge data could be well scaled by the velocity and the atomic number of an incident ion.

So far, there are several reviews on the experimental and theoretical results on the CSD and the average charge [7]. Experimental data were well compiled by several authors [1,8]. Several empirical scaling formula for the average charges were presented for the single-particle incidence. Bohr [9] presented a simple formula based on the velocity-stripping criterion, where the average charge q of the ion with atomic number Z is proportional to the ion velocity V as long as q is less than half of Z. In order to get a formula applicable up to higher velocities, Betz extended Bohr's formula by considering the velocity distribution of the bound electrons in the Thomas-Fermi model [10]. From an empirical data fitting, Dmitriev and Nikolaev [11] proposed a velocity-dependent formula which is different from these two models. In close atomic collisions at relatively low collision energies, Meron and Rosner [12] presented a compound-atom model for the CSD. Here the CSD is assumed to be in equilibrium even in a single collision with a target atom.

Apart from monoatomic ions, recent interest has been focused on the high-energy polyatomic ions, or, cluster projectiles. Ion clusters and highly charged biomolecules have been accelerated at high energies (e.g., 10 MeV–1 GeV) [13]. There will be new phenomena taking place in electronic excitations. One of our interest is the dependence of the induced electron excitation and related phenomena on the number of ions in the cluster. The subjects to be studied in this field are wide ranging: fragmentation of the clusters [14–16], breakup due to the Coulomb explosion [17], energy loss or energy deposition in a target [18–22], and cluster multiple ionization [23]. In these phenomena, the resultant effects induced by the incident cluster are expected to be much stronger than those by a single ion, due to strong spatial correlations in the electron excitation. There the average charge of the projectile inside a target plays the main role. Quite recently, a very remarkable result was reported on the cluster average charge by Brunelle *et al.* [24]. They found that the average charges per ion of the MeV carbon cluster ions C_n^+ ($n=3-10$) transmitting carbon foils were significantly lower than those of single ions with the equivalent kinetic energy per atom. They also found that this diminution of the average charge was enhanced with increasing the number of constituent atoms in the cluster. Moreover, as the foil thickness increases, this effect tends to vanish and the cluster average charge per ion approaches the single-particle

average charge with the equivalent velocities. This was our motivation to investigate whether it is possible to reconcile the cluster effect problem between the energy loss and the average charge in the carbon-cluster impact phenomena [25]. As for the reduction of the cluster average charge, several works were recently presented [26–29]. The basic treatment of the work [28] is an application of the Brandt-Kitagawa model [30]. The atom correlation of the cluster in matter was simulated [29]. As for the energy loss, they treated N_2 molecular-ion incidence [28].

The aim of the paper is to present a theory of the cluster average charge in the bulk, which is able to explain the results by Brunelle *et al.*, and to reconcile, in practice, the cluster effect in the average charge with the cluster effect in the energy loss. Here we develop our theory on the background that the cluster average charge is described within the same framework as the single-ion average charge, except for special remarkable points needed in the cluster case. We have to be able to consistently explain the average charges not only of the single ion, but also of the cluster. Moreover, the bulk average charge of the cluster should be connected with the energy loss in the bulk. In Sec. II, the present theories on the cluster-average charge and on the cluster energy loss are described in detail. Section III is devoted to presenting the numerical results, comparison with the experimental data, and discussion. Throughout this paper, m, e, and $\hbar$ denote, respectively, the electron rest mass, the elementary charge, and the Planck constant divided by 2π. In addition, we use the Bohr radius and the Bohr velocity denoted by $a_0=\hbar^2/me^2=0.529\times10^{-10}$ m and $v_0=e^2/\hbar=2.19\times10^6$ m/s.

II. THEORY

Here we present a theory that can give the average charges of not only the single-particle ions, but also of the cluster ions on the same theoretical background. First, we start with considering the case of the single particle penetrating a foil. After that, the case is considered of the cluster incidence, in which both the effect of surrounding ions and the self-consistency are needed to determine the average charge of each constituent ion. After stating the Coulomb explosion process, we finally give the cluster-energy-loss formula in the dielectric formalism.

A. Average charge of a single ion in a foil

First we consider the stripping rate of the bound electrons on the projectile of atomic number Z moving with velocity $\vec{V}$ inside a solid foil. Let us denote by $\vec{v}$ the velocity of a bound electron on the projectile at rest. When the projectile enters a solid foil, the bound electrons undergo collisions with the target electrons and/or nuclei and some of them will be excited or stripped off. Here we adopt the fluid-mechanical picture, in which the flow velocity experienced by such bound electrons is $-\vec{V}$ in the rest frame of the projectile. Therefore, the velocity of such an excited electron changes from $\vec{v}$ to $\vec{v}-\vec{V}$ in the rest frame of the projectile. Thus, the excitation occurrence will be restricted to the case where the following energy condition is fulfilled:

$$\tfrac{1}{2}n(\vec{v}-\vec{V})^2>\tfrac{1}{2}mv^2+I. \tag{1}$$

Here I denotes the activation energy to be applied to various cases. The velocity distribution function $f(\vec{v})$ of the electrons in a neutral atom with atomic number Z is determined by the maximum entropy principle under the conservation of the total number Z of electrons and the total kinetic energy E, where

$$Z=\int d\vec{v}\, f(\vec{v}), \quad E=\int d\vec{v}\, \tfrac{1}{2}mv^2 f(\vec{v}). \tag{2}$$

Introducing the Lagrange undermined multiplier method, we seek a function $f(\vec{v})$ that makes maximum the following quantity W:

$$W=-\int d\vec{v}\, f(\vec{v})\ln f(\vec{v})+c_1\left\{Z-\int d\vec{v} f(\vec{v})\right\} +c_2\left\{E-\int d\vec{v}\,\tfrac{1}{2}mv^2 f(\vec{v})\right\}. \tag{3}$$

Here c_1 and c_2 are the undermined constants. After some algebra, we finally obtain the solution

$$f(\vec{v})=Z\left(\frac{a}{\pi}\right)^{3/2}\exp(-av^2), \tag{4}$$

together with $a=3/(2\langle v^2\rangle)$ and

$$\langle v^2\rangle=\frac{1}{Z}\int d\vec{v}\, v^2 f(\vec{v}). \tag{5}$$

Next, let us evaluate $\langle v^2\rangle$. The total kinetic energy E_k of electrons in the atom is statistically evaluated as

$$E_k=A\frac{Z^{5/3}}{\Lambda^2}\left(\frac{e^2}{a_0}\right), \tag{6}$$

using the Thomas-Fermi-Moliere (TFM) electron distribution

$$\rho(\vec{r})=\frac{Z}{4\pi r}\sum_{j=1}^{3}\alpha_j\left(\frac{\beta_j}{\Lambda}\right)^2\exp\left(-\frac{\beta_j r}{\Lambda}\right). \tag{7}$$

In the above equation, the values of parameters are $\alpha_1=0.10$, $\alpha_2=0.55$, $\alpha_3=0.35$, $\beta_1=6.0$, $\beta_2=1.20$, $\beta_3=0.30$, and the screening length is given by $\Lambda=0.8853Z^{-1/3}a_0$. The constant A is expressed as

$$A=\frac{3}{10}\left(\frac{3\pi}{4}\right)^{2/3}\int_0^\infty dt\, t^{1/3}\left[\sum_{j=1}^{3}\alpha_j\beta_j^2\exp(-\beta_j t)\right]^{5/3}=0.4279.$$

Here we can prove the virial theorem, i.e., $E_k=-\frac{1}{2}(E_{ee}+E_{ne})$, where E_{ee} and E_{ne} denote the electron-electron interaction and the nucleus-electron interaction, respectively. Then we have the total energy $E_{\text{total}}=E_k+E_{ee}+E_{ne}=$

$-E_k$. From the expression (6), the average kinetic energy per electron is straightforwardly found to be

$$E_b = E_k/Z = 0.546Z^{4/3}\left(\frac{e^2}{a_0}\right). \tag{8}$$

Here we should connect E_b with $\frac{1}{2}m\langle v^2\rangle$. Therefore the root-mean-square velocity per electron reduces to the average velocity V_b of the bound electrons in a single atom such as

$$\sqrt{\langle v^2\rangle} = V_b = \sqrt{2E_b/m}v_0 = 1.045Z^{2/3}v_0. \tag{9}$$

Up to here, we determined the physical parameter $a = 3/(2V_b^2)$ that governs the velocity distribution [Eq. (4)] of the bound electrons in an isolated atom. The average charge Q of the isolated atom can be evaluated by counting the number of electrons stripped off from the atom after scattering. Then we have the following expression:

$$Q = \int d\vec{v}\{f(\vec{v}) - f(\vec{v}-\vec{V})\}. \tag{10}$$

The integration above should be performed only in the region of $\vec{v}$ that fulfills the condition $f(\vec{v}) \geqslant f(\vec{v}-\vec{V})$ together with Eq. (1). After evaluating the integration, one finally has the following expressions with $V_I = \sqrt{2I/m}$:

$$Q/Z = \tfrac{1}{2}P(y_-, y_+) \quad \text{for } V < V_I, \tag{11}$$

and

$$Q/Z = \tfrac{1}{2}[P(0,y_-) + P(0,y_+)] \quad \text{for } V > V_I, \tag{12}$$

where

$$y_- = \sqrt{\frac{3}{8}}\frac{|V_I^2 - V^2|}{VV_b}, \quad y_+ = \sqrt{\frac{3}{8}}\frac{V_I^2 + V^2}{VV_b}, \tag{13}$$

and

$$P(x,y) = \frac{2}{\sqrt{\pi}}\int_x^y dt\, \exp(-t^2). \tag{14}$$

When $I = 0$ (i.e., $V_I = 0$), Eqs. (11) and (12) reduce to

$$Q/Z = P(0,y) \tag{15}$$

with

$$y = \sqrt{\frac{3}{8}}\frac{V}{V_b}. \tag{16}$$

B. Average charge of a cluster ion in a foil

In this section we present the average charge theory for the cluster ions in a foil, which was developed on the theoretical basis given above. Our motivation to solve the problem is inspired by the molecule binding energy. As the simplest example, let us consider the H_2^+, where the electron is bound by two protons. This is a typical example of the so-called two-center problems. As is well known, the ground-state energy of an electron in a hydrogen atom at rest in vacuum is -13.6 eV. On the other hand, the ground-state energy of an electron in H_2^+ is about -28 eV [31] (the nuclear-nuclear repulsion energy is not taken into account). This enhancement of the electron binding energy is due to one more proton participating in binding the electron more strongly. One can see from this example that the more the number of the Coulomb attractive centers existing, the stronger the binding effect acting on the electron becomes. This conjecture is generally valid for the ground-state configuration so that we can expect the cluster projectile to be treated in this way. Thus the problem is reduced to how to involve the effect of neighboring ions around a given ion. One simple and practical prescription is to estimate the extra interaction energy between the electrons on the host ion and the surrounding ions.

According to the perturbation treatment, the surrounding ions can affect the electron binding energy, and quantum mechanically speaking, it will be estimated as a shift of the energy level considered. In order to make the treatment simple, let us suppose only one ''impurity'' ion with atomic number Z_2, and N_2 electrons located at a distance R from the host ion at the origin, since generalization to many ''impurity'' ions is straightforward. Now we assume the host ion with atomic number Z binds N electrons, the spatial distribution of which is described by the modified TFM distribution as

$$\rho(\vec{r}) = \frac{N}{4\pi r}\sum_{j=1}^{3}\alpha_j\left(\frac{\beta_j}{\Lambda}\right)^2\exp\left(-\frac{\beta_j r}{\Lambda}\right), \tag{17}$$

where Λ is the size parameter of the electron cloud. Let us evaluate the interaction energy ΔU between the impurity ion and the electron on the host ion. The formal expression is given by

$$\Delta U(R) = -e^2\int d\vec{r}\,\rho(\vec{r}+\vec{R})V(\vec{r}), \tag{18}$$

where $V(\vec{r})$ denotes the electric scalar potential created by the partially stripped impurity ion. In the TFM form, one has

$$V(\vec{r}) = \frac{Q_2}{r} + \frac{Z_2 - Q_2}{r}\sum_{j=1}^{3}\alpha_j\exp\left(-\frac{\beta_j r}{\Lambda_2}\right) \tag{19}$$

with $Q_2 = Z_2 - N_2$ and Λ_2 is the size parameter of the impurity ion. After carrying out the integration, we finally obtain

$$\Delta U(R) = -\frac{NQ_2e^2}{R}\sum_{j=1}^{3}\alpha_j\left\{1-\exp\left(-\frac{\beta_j R}{\Lambda}\right)\right\} - \frac{NN_2e^2}{R} \times\sum_{j=1}^{3}\sum_{i=1}^{3}\alpha_j\alpha_i\frac{\exp\left(-\frac{\beta_i R}{\Lambda}\right) - \exp\left(-\frac{\beta_j R}{\Lambda_2}\right)}{\left(\frac{\Lambda}{\Lambda_2}\right)^2\left(\frac{\beta_i}{\beta_j}\right)^2 - 1}. \tag{20}$$

It is natural that the separation R between the host and the impurity is usually larger than the size parameters Λ and Λ_2 of the electron clouds, Eq. (20) reduces to the result of the point-charge model: $\Delta U(R) = -NQ_2e^2/R$. This result is straightforwardly extended to the case where an arbitrary number of impurity ions exist around the host ion. Then summing up the contributions of the individual surrounding ions, we have a more general expression

$$\Delta U = -N\sum_i \frac{Q_i e^2}{R_i}, \tag{21}$$

where R_i denotes the distance between the host ion and the ith ion with charge $Q_i e$. The quantity (21) is the interaction energy added to the binding energy for an isolated ion [Eq. (8)]. As a consequence, the influence of the surrounding ions gives rise to the increase in the average binding energy per electron of the host ion as follows:

$$E_b = 0.546Z^{4/3}\frac{e^2}{a_0} + \frac{|\Delta U|}{N}. \tag{22}$$

This modified binding energy E_b plays a key role in the cluster-average-charge theory. As is the same as for the single-ion incidence, we can develop the theory on the basis of the fluid-mechanical model. Here what we have to do is to replace the E_b in Eq. (8) by the expression of Eq. (22). This replacement leads us, instead of V_b in Eq. (9), to the following modification:

$$V_{b,m} = \left(2\times 0.546Z^{4/3} + \sum_i 2Q_i/r_i\right)^{1/2} v_0, \tag{23}$$

where $r_i = R_i/a_0$.

Now we can arrive at the theoretical formula for the cluster average charge. For convenience, let us summarize the derived formula in somewhat abbreviated form. The average charge Q_i of the ith ion located at position R_i with atomic number Z_i is given by

$$Q_i/Z_i = P(0,y_i), \tag{24}$$

with

$$y_i = \left(\frac{3}{8}\right)^{1/2}\frac{V}{V_{b,i}}, \tag{25}$$

$$V_{b,i} = \left(1.092Z_i^{4/3} + \sum_{j(\neq i)}\frac{2Q_j}{|\vec{r}_j - \vec{r}_i|}\right)^{1/2} v_0. \tag{26}$$

It is noted that the summation in Eq. (26) should be taken over the surrounding (excluding the ith ion) ions. These results Eqs. (24)–(26), present the very important aspect that the average charge of each ion depends on both the average charges of other ions and their positions. It means that even for diatomic molecular ions the average charge will be different from the single atom at equivalent velocities. There arises the question of how the average charge per ion varies by increasing the number of constituent atoms in the cluster and depending on the spatial structures, etc. We will give answers to these questions in Sec. III

C. Self-consistent calculation

Before going to numerical estimation, we would like to briefly summarize the result. First, we presented the average-charge value of the single ion in a material, based on the fluid-mechanical model. The kinematic parameter for the single-ion incidence is solely the ion velocity V. As for the cluster incidence, on the other hand, not only the ion velocity, but also its structure becomes important. At the same time, the average binding energy per electron, which is the characteristic parameter in the theory, reflects the structure-dependent binding effect of surrounding ions in the cluster. Let us determine the average charge of the cluster ions, composed of n atoms. The average charge Q_i of the ith constituent ion is determined by the average binding velocity $V_{b,i}$, while the $V_{b,i}$ includes the average charges, i.e., $Q_1, Q_2, \ldots, Q_{i-1}, Q_{i+1}, \ldots, Q_n$, of all other constituent ions. Therefore, Q_i can be symbolically written as a function of $Q_1, Q_2, \ldots, Q_{i-1}, Q_{i+1}, \ldots, Q_n$ as

$$Q_i = Q_i(Q_1, Q_2, \ldots, Q_{i-1}, Q_{i+1}, Q_{i+2}, \ldots, Q_n)$$
$$(i = 1,2,3,\ldots,n).$$

This means that a set of Q_i's must be determined self-consistently. Moreover, due to the Coulomb explosion, the mutual distances of ions evolve with the dwell time in a foil, or the penetration depth (here we assume the ion trajectory to be a straight line). Then Q_i's are also the implicit functions of the penetration depth. To solve the above equation, an iterative calculation must be done till all the computed values are convergent enough. In practice, we confirmed that the calculated Q_i's were convergent within 1% accuracy when the iteration was repeated seven times. As will be seen later, this accuracy is enough to discuss the foil thickness dependence of the cluster average charge. Finally we emphasize that this self-consistent method can rather precisely predict the average charge of the cluster in the bulk even in the case where the internal Coulomb forces act on the cluster itself.

In order to derive a characteristic cluster average charge, we define the average charge per ion, $Q(n)$, for the cluster C_n by

$$Q(n) = \left(\sum_{i=1}^{n} Q_i\right) \Big/ n. \tag{27}$$

Later this quantity will be compared with the average charge $Q(1)$ of a single C ion. As shown in Sec. III, $Q(n)$ is always smaller than $Q(1)$ in relatively thin foils, and $Q(n)$ approaches $Q(1)$ with increasing foil thickness. We just call the former feature the cluster effect in the average charge.

D. Expansion of a cluster—Coulomb explosion

In general, as the swift polyatomic projectile enters the target material, the bonding electrons will be stripped off and constituent atoms in a cluster are positively charged in a thin

TABLE I. Values of F against n.

n	2	3	4	6
F	2	3	$\frac{4+\sqrt{2}}{2}$	$\frac{5}{4}+\frac{\sqrt{3}}{3}$

region (a few nanometers for the MeV/atom ions). Then takes place the so-called Coulomb explosion process that converts the internal repulsive potential energy into the kinetic energies of the constituent ions, keeping the total energy constant in the center-of-mass frame. For two-atom (ion) systems, by solving the Newtonian equation, the expansion rate of the mutual distance R can be obtained analytically [32]. On the other hand, for a polyatomic system, it is impossible to obtain analytical solutions except for special cases. In a special system, however, we can obtain the analytical solution as follows. Let us consider the homonuclear polyatomic projectile where all ions have the same average charge Q and the same mass M. In addition, the structure is highly symmetric, i.e., a ring structure on a plane with the equal nearest-neighbor distance R. In this case, the time evolution of R can be analytically solved as

$$\tau=\sqrt{\xi}\sqrt{\xi-1}+\ln(\sqrt{\xi}+\sqrt{\xi-1}),$$

where $\tau=t/t_0$ and $\xi=R/R_0$ are the reduced time and the reduced separation, respectively, and R_0 is the initial nearest-neighbor distance. The characteristic time is defined by $t_0=[R_0^3M/(2FQ^2)]^{1/2}$, where the factor F depends on the number n of atoms in the projectile and on their structure such as

$$F=2\left|\sin\left(\frac{\pi}{n}\right)\right|^3\sum_{i=1}^{n-1}\frac{1}{\left|\sin\left(\frac{i\pi}{n}\right)\right|}.$$

In Table I, we tabulate the values of F for several ring structures.

We would like to treat the motion of more than three atoms so that the expansion rate of the mutual distances is estimated by means of a molecular-dynamics simulation. If the stochastic fluctuations are all neglected, the motion of the Coulomb expansion would be uniform. Then the relative distance R_{ij} of a given pair of ions in the cluster will be governed by the conversion process of the initial electrostatic potential energy q_iq_j/R_{ij} with $R_{ij}=|\vec{R}_i-\vec{R}_j|$ into the kinetic energy of the relative motion. It is obvious that this process is independent of the elastic collision between the projectile and the target atom. Thus the Coulomb explosion is the main mechanism of the self-expansion (or self-destruction) of the cluster in the foil. We assume here the bare Coulomb interactions since swift ions with velocities greater than the Fermi velocity ($\approx 1.3v_0$ for the carbon target) cannot be screened, or, even if so, screened only a bit, by the conduction electrons.

E. Electronic energy loss of a cluster in a foil

We describe the electronic energy loss of cluster ions in a foil. Our scenario is the following.

(1) The foil is devided by thin computational layers. The lost energy in the lth layer is given by $\Delta E_l=NS_l\Delta x_l$, where N, S_l, and Δx_l denote, respectively, the number density of target atoms, the electronic stopping cross section for the cluster, and the thickness of the lth layer.

(2) The constituent atom positions and their velocities are input first, and their average charges are calculated self-consistently. Next, the electronic stopping cross section is calculated under this spatial configuration of the cluster. The cluster is assumed to be randomly oriented so that the data on the relative distances are only significant in the energy-loss calculation. This is a series of the computation cycle.

(3) In the next computational layer, the expanded interionic spacings due to Coulomb repulsive forces are first estimated by employing the Runge-Kutta method. After that, the self-consistent average charges and the energy loss of the expanded cluster are calculated in the similar manner as the previous step.

(4) By repeating the above computation cycle layer by layer, we finally obtain the total energy loss of the cluster after passing through the foil.

In the above energy-loss estimation, the key role in the energy loss is played by the electronic stopping cross section S for the cluster. There contribute two kinds of electronic excitations, i.e., the core-electron excitation and the conduction-electron excitations. In order to estimate S, we adopt the wave-packet treatment [33], where both excitations are treated in the dielectric-function formalism. So far, this method provided fruitful results on the electronic stopping cross section of gaseous and solid targets not only for single ions, but also for molecular ions over a wide energy range. The excitation of conduction electrons is characterized by the random-phase approximation dielectric function, while the core excitation is characterized by the new dielectric function, derived for the Gaussian occupation probability [33]. Apart from those explicit forms, we start with the formal expression of the dielectric function $\epsilon(k,\omega)$, which is common to both excitations. Then the electronic stopping cross section for the cluster S is given as follows:

$$S=\frac{1}{2\pi^2V}\int\frac{d\vec{k}}{k^2}|\rho_{\rm ext}(\vec{k})|^2\int d\omega\,\omega\,{\rm Im}\left[\frac{-1}{\epsilon(k,\omega)}\right]\delta(\omega-\vec{k}\cdot\vec{V}). \tag{28}$$

Here $\rho_{\rm ext}(\vec{k})$ denotes the Fourier transform of the cluster charge density $\rho_{\rm ext}(\vec{r})=e\Sigma_i[Z\delta(\vec{r}-\vec{R}_i)-\rho_i(\vec{r}-\vec{R}_i)]$, where $\vec{R}_i$ is the position vector of the ith ion in the center-of-mass frame of the cluster moving with constant velocity $\vec{V}$ in the material, and $\rho_i(\vec{r}-\vec{R}_i)$ denotes the spatial distribution of electrons attached to the ith ion. In this expression, the cluster charge density is assumed to be given by the overlap of isolated partially stripped ions. In addition, we explicitly take into account neither the cluster orientation nor the anisotropy of $\rho_i(\vec{r}-\vec{R}_i)$. Therefore the quantity $|\rho_{\rm ext}(\vec{k})|^2$ is replaced by its orientation average

$$\langle|\rho_{\rm ext}(\vec{k})|^2\rangle = e^2\sum_i \left[\{Z-\rho_i(k)\}^2 + \sum_{j(\neq i)}\{Z-\rho_i(k)\} \times\{Z-\rho_j(k)\}\frac{\sin(kR_{ij})}{kR_{ij}}\right],$$

where R_{ij} is the relative distance between the ith and the jth ions. Here $\rho_i(k)$ is the Fourier transform of the spherically averaged $\rho_i(\vec{r})$. Here in order to describe rather reasonably and without complexity, we adopt the Thomas-Fermi-Moliere-type distribution with atomic number Z and N bound electrons. One finally obtains with the screening constant $\Lambda = 0.6269N^{2/3}a_0/(Z-N/7)$ the following expression (see the Appendix):

$$\rho(\vec{k}) = N\sum_{j=1}^{3}\frac{\alpha_j\beta_j^2}{\beta_j^2+\Lambda^2k^2}. \tag{29}$$

As the target material is assumed isotropic, we rewrite S in Eq. (28) as

$$S = \frac{2}{\pi V^2}\int_0^\infty\frac{dk}{k}\int_0^{kV}d\omega\,\omega\,{\rm Im}\left[\frac{-1}{\epsilon(k,\omega)}\right]\langle|\rho_{\rm ext}(\vec{k})|^2\rangle. \tag{30}$$

The expressions (28) and (30) hold sound in the adiabatic case where the time evolution of the internal motion (e.g., the coulomb explosion) is slow enough, compared with that of the center-of-mass motion. This is the case considered in this paper. The stopping cross section S per atom in Eq. (30) is given by the sum of the partial shellwise stopping cross sections. More details of this calculation method are described in another paper [34].

In general, the stopping cross section for the cluster and the resultant energy loss are different from the corresponding quantities for the single ion multiplied by the number of atoms in the cluster. This is caused by the interference terms in the $\langle|\rho_{\rm ext}(\vec{k})|^2\rangle$. Such a difference in the stopping for the cluster and for the single ion is called the cluster effect in the energy loss. To investigate this effect, it is convenient to compare the energy loss $\Delta E(n)$ of a penetrating C_n cluster with the energy loss $\Delta E(1)$ of the single C ion at the equivalent velocity. So far, two standards have been adopted: one is the absolute difference in the energy loss per ion, RE_1, defined by

$$RE_1 = \Delta E(n)/n - \Delta E(1), \tag{31}$$

and the other is the relative ratio of the energy loss per ion, RE_2, defined by

$$RE_2 = \Delta E(n)/[n\Delta E(1)]. \tag{32}$$

We recognize that the positive (negative) cluster effect appears when $RE_1>0$ ($RE_1<0$) or $RE_2>1$ ($RE_2<1$). In the following section, the calculated results are presented along this line, and compared with the recent experimental data.

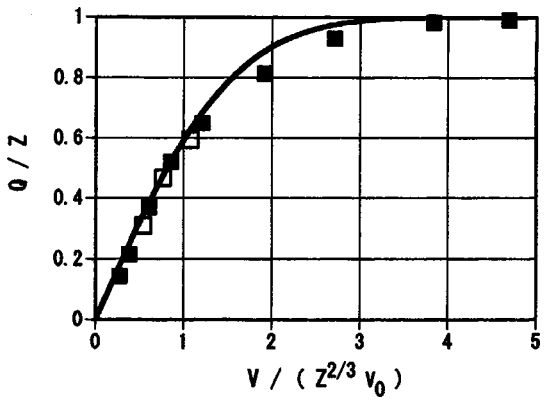

FIG. 1. Fractional average charge Q/Z as a function of the reduced ion velocity $V/(Z^{2/3}v_0)$ for single carbon ion in carbon foil: present result (solid line) and the data obtained by Shima *et al.* [8] (solid squares) and by Brunelle *et al.* [24] (open squares).

III. RESULTS AND DISCUSSION

In this section, we show the theoretical results both on the cluster average charge and on the cluster energy loss, and compare them with the recent experimental data. First, we show the average charge of the single ion in foils. As a general feature, the average charge Q of the single ion with atomic number Z depends very weekly on the target material, and solely on the ion velocity V. This is a widely and commonly known result. Moreover, the average charge for various monoatomic ions is also well known to be scaled by a statistical parameter [1,8]. This is the background in which we present the statistical picture, where the average orbital velocity per electron is characterized by the factor $Z^{2/3}v_0$. Now the fractional average charge Q/Z is well scaled as a function of the ion velocity V divided by $Z^{2/3}\nu_0$, as expected from Eqs. (9),(15), and (16). Figure 1 shows this fact for the single carbon ion penetrating carbon foils. The experimental data are cited from the papers of Shima *et al.* [8] and Brunelle *et al.* [24]. Here we do not cite much experimental data in order to especially compare in detail the cases of carbon ions and also to avoid complexity. The agreement between the theoretical and the experimental results is rather good over a wide range of velocity, though the calculated values are a bit larger than the data around at the reduced velocity $V/Z^{2/3}\nu_0=2$. Especially, the data obtained by Brunelle *et al.* [24] almost completely coincide with the theoretical ones. Before the calculation of the cluster average charge, we comment on the structure of carbon cluster C_n. As is known, the carbon clusters have several structures [35,36], i.e., linear chain, ring, and fullerene. Roughly speaking, the clusters with a relatively small number of atoms tend to have the linear-chain structures, and with increasing the number of atoms they tend to have the ring structures. The symmetry notation reported for the linear-chain structure is $D_{\infty h}$, and those for the ring structures are D_{2h} for C_4, D_{3h} for C_6, D_{4h} for C_8, and D_{5h} for C_{10}. We set the nearest-neighbor distance in the linear-chain structure as $2.4a_0$. In addition to these structures, computation was carried out as a trial for the D_{3h} structure for C_8, and the D_{10h} structure for C_{10}, though these have not been reported as far as the author

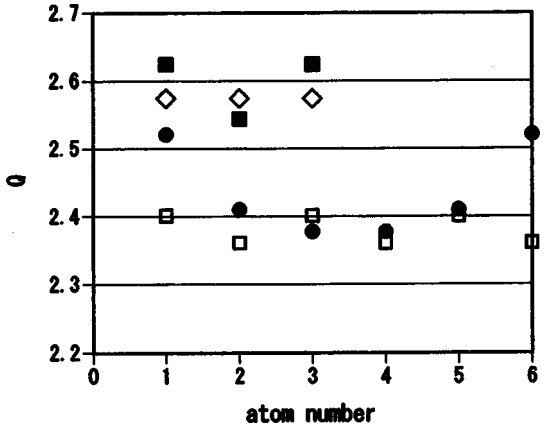

FIG. 2. The self-consistently calculated average charge Q of constituent atoms in the C_n cluster with the kinetic energy 2 MeV/atom, penetrating the carbon foil of 2.39 μg/cm^2 thickness: solid squares ($n=3$, linear-chain structure), open diamonds ($n=3$, triangle structure), solid circles ($n=6$, linear-chain structure), open squares ($n=6$, ring structure) (see text).

knows. Here we would like to give two comments. One is that the single bonds and the double bonds are not distinguished. The other is that the electron distribution of a cluster is assumed to be the overlap of the constituent atoms. Under these assumptions, we obtained the numerical results shown hereafter.

Figure 2 shows the average charge of the individual ions calculated self-consistently for the carbon cluster C_n with the kinetic energy $E=2$ MeV/atom penetrating a foil of thickness 2.39 μg/cm^2. Here we assume two structures: for the C_3 cluster, the linear-chain and the triangle D_{3h} structures with the nearest-neighbor distance $d=2.4a_0$, and for the C_6 cluster, the linear-chain with $d=2.4a_0$ and the ring D_{3h} structure with $d=2.488a_0$ [35]. In order to hold self-consistency, calculation of the average charges for individual ions is iterated about ten times till the values converge under a given cluster structure. The atoms in the C_n cluster are numbered from 1 to n in order. For the linear-chained clusters, this numbering was done from one end to another end. The abscissa in Fig. 2 indicates the atom number in the clusters, given in this way. For the C_3 with the triangle structure, each ion plays an equivalent role so that all average charges are completely equal, as one can easily understand from the spatial symmetry. On the other hand, for the C_3 with the linear-chained structure, the central ion is most strongly affected by the field of two other surrounding ions so that its average charge is the lowest among them. On the contrary, the ions at the edges of linear clusters have the largest average charges since the binding effect works minimum. Regarding the ring C_6, the spatial symmetry is D_{3h} so that six atoms are classified into two equivalent groups. Thus there appear two values of the average charges in the ring structure. In our treatment, the average charges strongly correlate with the spatial symmetry of the cluster.

Figures 3(a)–3(d) show the cluster average charge per ion, $Q(n)$, for the 2 MeV/atom $C_n(n=3,5,8,10)$ clusters versus the thickness of the carbon foil ranging from 2.2 to 40 μg/cm^2, where $Q(n)$ was calculated as in Eq. (27). The value of $Q(1)$ is equal to the value of Q in Fig. 1 at the corresponding velocity. In each figure, the solid line and the broken line are the theoretical results for the C_n cluster with

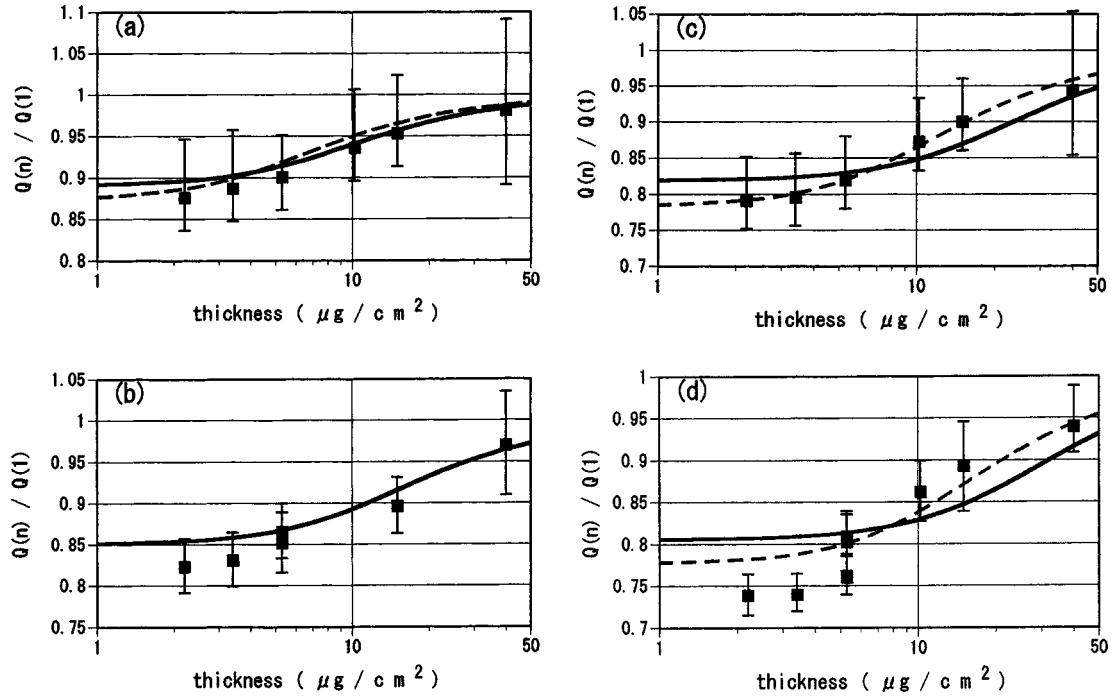

FIG. 3. (a)–(d) The foil-thickness dependence of the average charge ratio, $Q(n)/Q(1)$, of the C_n with the kinetic energy 2 MeV/atom, emerging from carbon foils: self-consistent calculation (solid line, linear-chain structure; broken line, ring structure) and the experimental data (solid squares with error bars) [24]: (a) $n=3$, (b) $n=5$, (c) $n=8$, (d) $n=10$.

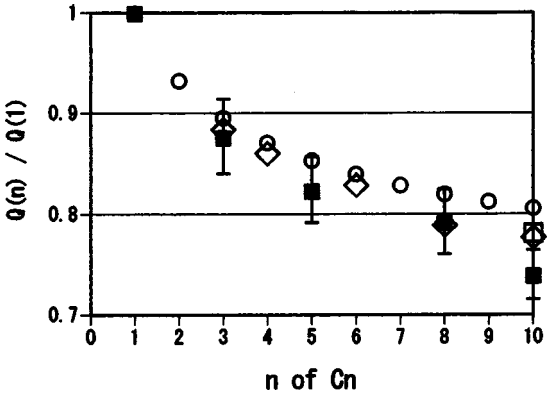

FIG. 4. The cluster-size dependence of the average charge ratio, $Q(n)/Q(1)$, of the C_n with the kinetic energy 2 MeV/atom emerging from the 2.2 μg/cm^2 carbon foil against the number of atoms, n, in the cluster: self-consistent calculation (open circles, linear-chain structure; open diamonds and open square ring structure) and the experimental data (solid squares with error bars) [24] (see text).

the linear-chain and the ring structures, respectively. The symmetries of the ring structures are D_{3h}, D_{4h}, and D_{5h} for the C_3, C_8, and C_{10} cluster, respectively. The solid squares with the error bars indicate the experimental data [24]. Each figure has a common trend that as the foil thickness increases, the $Q(n)$ values gradually approach the $Q(1)$ value. The asymptotic relation $Q(n)/Q(1)=1$ implies the vanishing of the spatial correlation among constituent ions of the cluster. In other words, those ions are separate enough from one another so that they behave as an ensemble of independent single ions. Judging from the magnitude of the error bars, we can say that the theoretical curves in both structures explain very well the trend of the experimental data. If we compare in more detail, the curves for the ring structures are in better agreement, as the cluster size n grows up. As for the C_{10} case, however, there is an exception that we discuss in detail. Different from the case of thicker foils, the $Q(n)/Q(1)$ values calculated in the linear-chain and ring structures are greater than the data at thin (less than about 6 μg/cm^2) foils. At thickness 5.3 μg/cm^2, the data are largely scattered so that it is not easy to say which is the most probable data. Moreover, the data look like changing abruptly at this foil thickness. As an attempt to elucidate this discrepancy, we again calculated the $Q(n)$ for the case of the stronger correlation, i.e., the D_{10h} ring structure, than the D_{5h} structure. As expected, the $Q(n)/Q(1)$ is lower than that of the linear-chained C_{10} by 0.03 at most. Moreover, there is only a few percent difference in $Q(n)$ of C_{10} between in the D_{5h} and in the D_{10h}. The experimental data, however, is still less than in the ring cases by about 0.03. Here, we may suggest one possibility to explain this discrepancy. It is the contraction of the ring along the direction of motion on entering a foil. This process would make the diameter of the cluster shorter than that of the initial ring. Then it leads to the stronger spatial correlation and the lower $Q(n)/Q(1)$ value.

Figure 4 shows the cluster-size dependence of the average charge ratio $Q(n)/Q(1)$ for the C_n cluster ions at the kinetic energy 2 MeV/atom, penetrating the 2.2 μg/cm^2 carbon foil. The calculated values are denoted by the open circles for the linear-chain structures, by the open diamonds for the D_{3h} at $n=3$, 6, for the D_{4h} at $n=4$, 8, and for the D_{5h} at $n=10$. In addition, the value for the D_{10h} at $n=10$ is denoted by the open square. The experimental data [24] are shown by the solid squares with error bars. At a glance, the theoretical trend on the n dependence of $Q(n)/Q(1)$ is quite consistent with the data. The most remarkable feature is the slowly decreasing relation with increasing the number of the atoms in the cluster. As for C_8 and C_{10}, the ring structures can better explain the data. For C_{10}, no significant difference was found between the D_{10h} and D_{5h} structures. In this figure, we can conclude that the calculated results are in rather good agreement with the data.

Here we would like to make some comments. In this research, we stress on the role of the variation of the binding energy due to the surrounding ions, and neglect the rearrangement of the electron distribution under the electric field of surrounding ions acting on. The validity of this insight is easily found if one is reminded of the perturbation treatment. According to it, the variation in the eigenenergy is the first-order contribution, while the normalization of the wave function is the second-order one [37]. This means that as far as the perturbation is concerned, the shift of the energy level is more preferential than the change of the spatial electron distribution. This is the reason why we focus on the energy variation as a leading effect. So far, two explanations have been made for the diminution of the molecular (e.g., H_2^+) average charge. One is the enhanced electron capture by a correlated small cluster *at the exit surface*, which was presented for low-velocity hydrogen ions. The other is the enhanced capture cross section *inside a solid* [38], presented for nitrogen ions. The electron-capture and the electron-loss processes compete to determine the average charge. We wonder how the electron loss is reconciled with the capture there. In this paper, we presented a direct method to determine the average charge of cluster ions in a bulk.

In spite of the present charge-state bulk process, somebody might point out the possibility of charge-changing process near and/or after the surface. In practice, for heavy ion projectiles, the post-foil ionization due to Auger decay were observed. However, this is not the true of light ions. If such a charge-changing surface effect takes place, the observed average charges are different from those inside a solid. In general, Auger decay enhances the charge of the emerging ion more than that of the ion inside a solid. The average charge of the projectile inside a solid is directly connected with the energy loss. In order to confirm our average-charge model more strictly, we also calculate the energy loss of the corresponding cluster ions. In the energy range studied here (more than a few keV/u), not the elastic collision process but the electronic excitation is the dominat energy-loss mechanism. The theoretical energy-loss formula we employed here is the wave-packet shell-by-shell method [33,34]. So far, this method brought us the stopping cross sections of materials, which are consistent with the available data not only for single ions, but also for molecular ions in frozen charge states or in the dissociating state.

Hereafter we focus on the energy loss of the clusters. A great concern is to what extent the reduction of the average

charge works in the energy loss. Figures 5(a)–5(g) show the calculated RE_1 [$\equiv \Delta E(n)/n - \Delta E(1)$] of the carbon-cluster ions at (a) $E=2.275$, (b) $E=2.436$, (c) $E=2.65$, (d) $E=2.95$, (e) $E=3.40$, (f) $E=4.15$, and (g) $E=5.65$ MeV/atom, penetrating the carbon foil of 25 nm thickness together with the experimental data. The total energy loss in a foil is estimated by the pileup of those in the computation layers of a few nanometers thickness. The Coulomb explosion process was successively incorporated layer by layer. The C_n clusters were assumed to have the linear-chain structures for $n=2-8$ and also the ring structures [35] for $n=3$, 4, 6, and 8. The cluster orientation was assumed random. In these figures, the open circles and the open diamonds denote the theoretical energy-loss values, respectively, for the linear-chain and for the ring structures, with the use of the present average charge theory (we call ''present'' model). The crosses denote the theoretical results under the assumption that the average charge of all ions in the cluster is equal to that of the single ion at the equivalent velocity, i.e., $Q(n)/Q(1)=1$ (we call ''old'' model). On the other hand, the solid squares with error bars indicate the experimental data [39]. From these figures, the old model presents a monotonic and saturated increase of RE_1 with increasing n, while the present model, yielding the maximum of RE_1 around $n=3$ or 4, gives quite a good agreement with the data. As is immediately understood, in comparison with the results in the old model, one finds the suppression of the RE_1 values, coming from the diminution of the average charge. Moreover, the values of RE_1 are still positive and the cluster effect can be predicted theoretically. This is valid in all cases of the kinetic energy presented. Let us move to the structure dependence of the RE_1 values. In the carbon foil of 25 nm thickness, the theoretical RE_1 values in the ring structures at $E=2.275$ MeV/atom are only a bit greater than in the linear-chain structures, while at $E=5.65$ MeV/atom they are seriously greater as the number of atoms in the cluster increases. However, the RE_1 values in the ring structures are still smaller than those predicted in the old model or the asymptotic average-charge case. Here we would like to note that in the energy-loss estimation, not only the magnitude of the average charge but also the structure of the cluster, or, the pair correlation of atoms in the cluster, play dominant roles. Thus we could find the remarkable result that the inclusion of the present model on the cluster average charge gives much better agreement with the experimental energy-loss data [39], and that though the cluster average charge per ion becomes smaller than the single-ion average charge, the energy loss per ion is still positive. Namely, the cluster effect in the energy loss is clearly recognized.

Up to here, we presented the positive cluster effect. On the other hand, one can also see the negative one. As an example of the lower incident energies, Fig. 6 shows the RE_1 values for the C_n with the kinetic energy $E=1.01$ MeV/atom, against n. The theoretical results at $n=3$, 4, 6, and 8 refer to the ring structure (denoted by the open diamonds) and others to the chain structure (denoted by the open circles). The solid squares with error bars denote the experimental data [20]. It is noted that the experimental RE_1 values are lower than the theoretical ones for the linear chains. However, if we assume the ring structures, agreement with the data becomes much better. At all events, the RE_1 values at this energy become negative, which is in contrast to the higher-energy cases as shown in Figs. 5(a)–5(g). The decreasing n dependence is theoretically found for the RE_1, which is in quantitative agreement with the data. The reason for this aspect originates from the fact that the contribution of the pair correlation works negative over the momentum-transfer region, which is dominant in the stopping S in Eq. (30).

In order to clearly indicate the positive and the negative characters, we present the velocity dependence of the RE_2 values in Figs. 7(a) and 7(b) for the linear-chained C_n ($n=2$, 3, 4, 6, 8, 10) and for the ring-structured C_n ($n=3$, 4, 6, 8, 10), respectively, penetrating the carbon foil of 26.5 nm thickness at the velocity V ranging from v_0 ($E=0.30$ MeV/atom) to $4.5v_0$ ($E=6.075$ MeV/atom). At the lower velocities, the RE_2 values for the ring structures are smaller than for the linear-chain structure, while at the higher velocities this relation is reversed. In fact, the RE_2 values for the ring C_n amounts to be 1.16–1.32 at $V=4.5v_0$, which are larger than the linear-chain case at the equivalent velocity. Let us define the threshold velocity $V_{\rm th}$ as the velocity at which the RE_2 curve crosses unity or the RE_1 curve crosses zero. Then one finds $V_{\rm th}=(1.9-2.4)v_0$ in the linear-chain clusters, and $V_{\rm th}=(2-2.8)v_0$ in the ring clusters. The latter case presents a wider variation in $V_{\rm th}$. These features also originate from the behavior of the pair-correlation function for the cluster. It is noticed that at the threshold velocity the pair-correlation function itself does not vanish but its contribution (the integration over the energy- and momentum-transfer region) vanishes. This is different from the case where the cluster atoms, penetrating a sufficiently thick foil, are fully dispersed and the pair correlation completely vanishes, resulting in $RE_1=0$ and $RE_2=1$.

In a final part, we would like to give some comments. The first is on the validity that we assume the immediate charge equilibrium to be accomplished on entering a foil. To discuss simply, let us consider the case of two charge components Q and $Q+1$ being dominant. Solving the rate equation, we define the charge equilibrium length $X_{\rm eq}$ by $X_{\rm eq}=1/[N(\sigma_{Q,Q+1}+\sigma_{Q+1,Q})]$. Here $\sigma_{Q,Q+1}$ and $\sigma_{Q+1,Q}$ denote the electron-loss and-capture cross section, respectively, and N is the number density of the target atoms. The charge Q is taken to be a value close to the equilibrium charge $Q_{\rm eq}$, e.g., $Q=3.0$ at $V=3v_0$. According to the Born approximation theory [5], the loss cross section $\sigma_{3,4}$ for a hydrogenlike ion at $V=3v_0$ colliding with a carbon atom is about 0.47×10^{-16} cm^2/atom. As $N=0.11\times10^{24}$ atoms/cm^3 for the carbon target, one can estimate $X_{\rm eq}\leqslant(N\sigma_{3,4})^{-1}=1.93$ nm. This length is much shorter than the foil thickness (25 nm) so that our assumption of the charge equilibrium being attained on entrance is not considered to be serious. Another comment is as for the wake effect. Now we assume the clusters to be in random orientation so that the wake effect on deformation of the cluster structure is not considered here. In other words, under the random orientation, it cannot discern which is the leading or the trailing ion. The more the number of the constituent ions in the cluster, the more difficult the

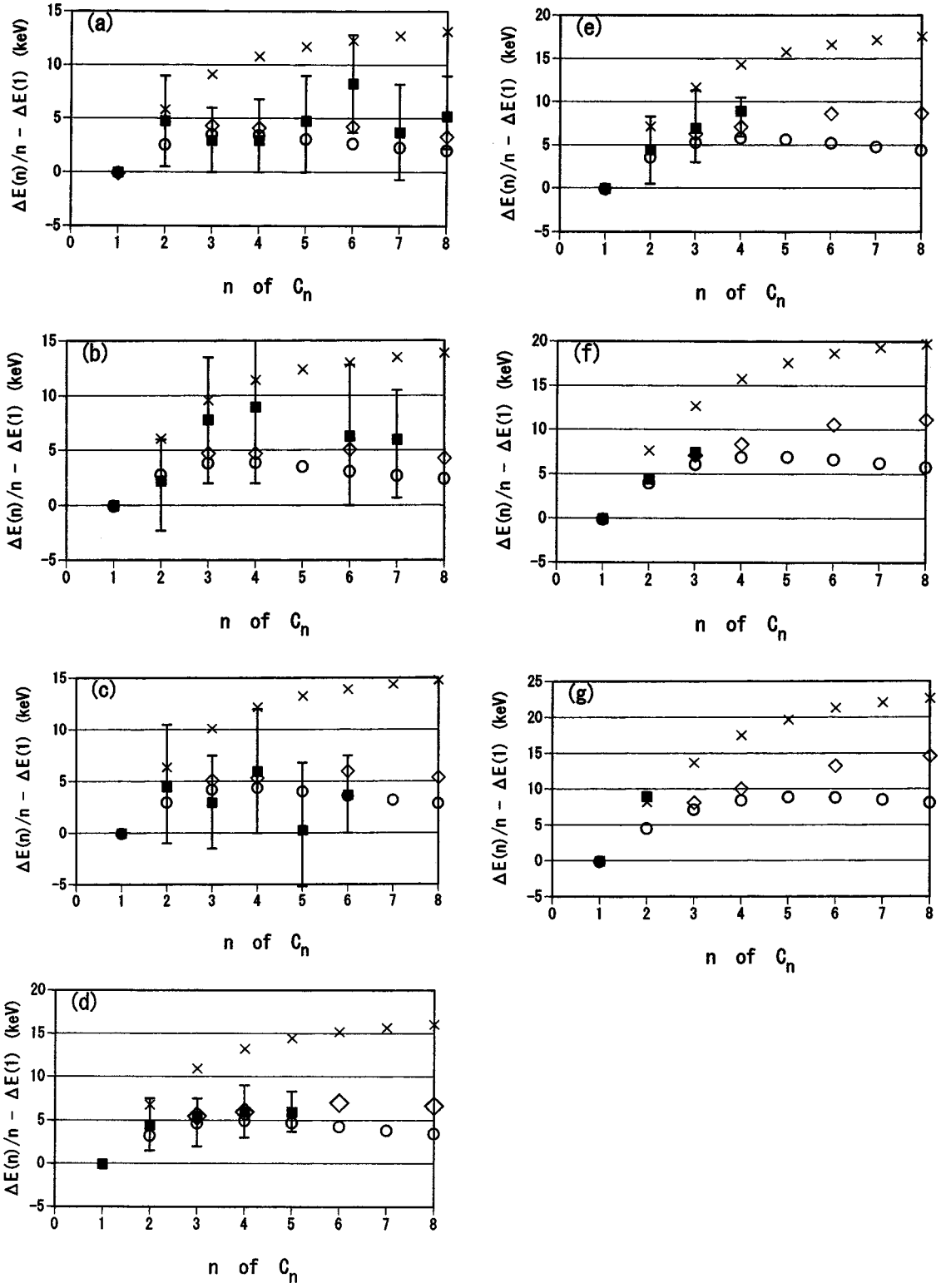

FIG. 5. (a)–(g) The cluster-size dependence of $RE_1 \equiv \Delta E(n)/n - \Delta E(1)$ in keV, against n of the C_n clusters penetrating the 25 nm carbon foil at the kinetic energy $E = 2.275$–5.65 MeV/atom: the theoretical results with the presented average-charge model (open circles, linear-chain structures; open diamonds, ring structures), the experimental data by Baudin *et al.* [39] (solid squares with and without error bars). For reference, the theoretical results with the assumption of $Q(n) = Q(1)$ for the linear-chained C_n are shown by the crosses (see text). (a) $E = 2.275$, (b) $E = 2.436$, (c) $E = 2.65$, (d) $E = 2.95$, (e) $E = 3.40$, (f) $E = 4.15$, (g) $E = 5.65$ MeV/atom (see text).

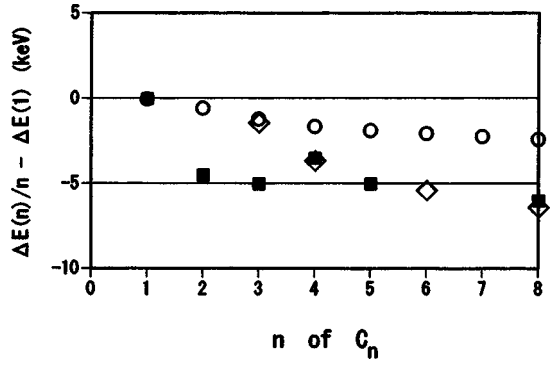

FIG. 6. The cluster-size dependence of $RE_1 \equiv \Delta E(n)/n - \Delta E(1)$ in keV, against n of the C_n clusters penetrating the 25 nm carbon foil at $E = 1.01$ MeV/atom: the theoretical results with the presented average-charge model (open circles, linear-chain structures; open diamonds, ring structures), the experimental data [20] (solid squares) (see text).

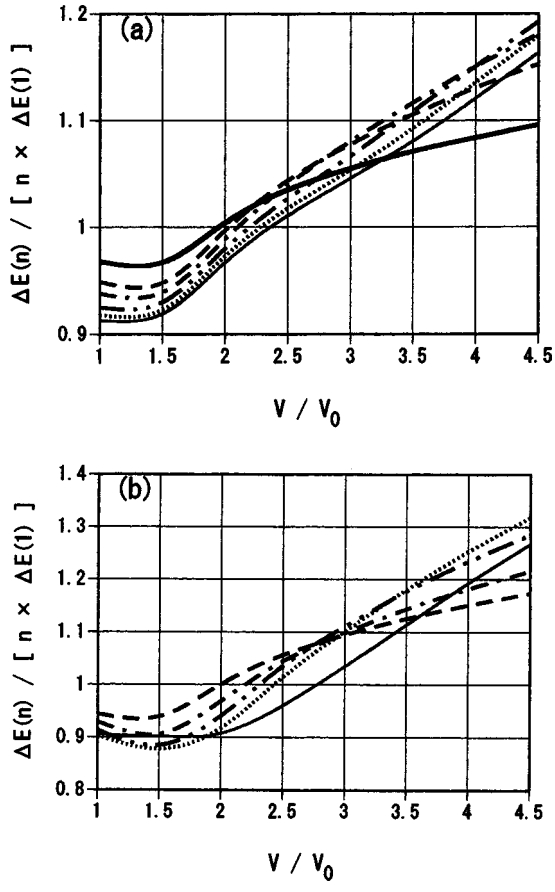

FIG. 7. (a) The velocity dependence of $RE_2 \equiv \Delta E(n)/[n\Delta E(1)]$, calculated for the linear-chain $C_n(n=2-10)$ clusters penetrating a carbon foil of 26.5 nm thickness at velocity $V = v_0 - 4.5v_0$: $n=2$ (thick solid line), $n=3$ (broken line), $n=4$ (dot-dashed line), $n=6$ (dot-dot-dashed line), $n=8$ (dotted line), and $n=10$ (thin solid line). (b). Same as in (a) except for the ring $C_n(n=3,4,6,8,10)$ clusters: $n=3$ (broken line), $n=4$ (dot-dashed line), $n=6$ (dot-dot-dashed line), $n=8$ (dotted line), and $n=10$ (thin solid line).

quantitative estimation of the wake effect becomes. Now, we think that the wake effect is not so serious since the induced wake waves with the wavelength $\lambda = 2\pi V/\omega_p$ [40] will interfere with each other and resultantly they are expected to cancel out or at least become weaker as a whole. Nevertheless, from more rigorous points of view, the effect of the induced charge on the cluster is still important. Our study of this effect is now in progress and the results will be presented in a forthcoming paper. One more comment is on the neglect of the edge effect, i.e., the neglect of the difference in time when the cluster atoms enter or exit a foil. This edge effect produces the time delay in the expansion of the ions. This time delay is estimated by $\tau_{\rm delay} = L_{\rm cl}/V$, where $L_{\rm cl}$ is the size of the cluster, which is much smaller than both the dwell time $\tau_{\rm dwell} = D/V$ and the characteristic time τ_0 of the Coulomb explosion, where D is the foil thickness. We found that, in this case, the successive ionization process gives only a negligibly small contribution to the Coulomb explosion.

In conclusion, a fluid-mechanical model with satisfying self-consistency is presented for the cluster average charge in the bulk. This average-charge theory will be applicable except for the cases where only a few quantum levels are significant, e.g., at very low velocities. It is remarkable that inspite of the reduction of the cluster average charge, we still can find the positive cluster effect in the inelastic energy losses in the bulk. This model can explain the measured average charges as well as the measured energy loss of the carbon clusters. In other words, our treatment reconciled the cluster average charge inside a solid with the cluster energy loss inside a solid. This means that the dominant charge-changing and electron excitation processes occur in the bulk rather than near the surfaces. In this way the recent experimental data on the cluster-impact phenomena are sufficiently meaningful and valuable. In future, further data on the cluster with the higher energies, obtained simultaneously both on the charge state and on the energy loss, will be expected to confirm this conclusion, and study further the interaction of the polyatomic ions with the materials.

ACKNOWLEDGMENT

This work was supported by a Grant-in-aid from the Japan Society for the Promotion of Science.

APPENDIX

Here we derive the expression (29) on the basis of a statistical method. Let us consider a partially stripped ion of atomic number Z, on which N electrons are bound. As a spatial distribution function, now we assume the Thomas-Fermi-Moliere type as

$$\rho(\vec{r}) = \frac{N}{4\pi r}\sum_{j=1}^{3}\alpha_j\left(\frac{\beta_j}{\Lambda}\right)^2\exp\left(-\frac{\beta_j r}{\Lambda}\right).$$

Here Λ is the screening parameter to be determined later. Now we calculate the kinetic energy E_k of the electrons, the

nuclear-electron interaction energy E_{ne}, and the electron-electron interaction energy E_{ee} as functions of the electron density $\rho(\vec{r})$ in the following:

$$E_k=\frac{3\hbar^2}{10m}(3\pi^2)^{2/3}\int d\vec{r}[\rho(\vec{r})]^{5/3}=A\frac{\hbar^2}{m}\frac{N^{5/3}}{\Lambda^2},$$

$$E_{ne}=-Ze^2\int d\vec{r}\frac{\rho(\vec{r})}{r}=-Be^2\frac{ZN}{\Lambda},$$

$$E_{ee}=\frac{e^2}{2}\int d\vec{r}\int d\vec{r}'\frac{\rho(\vec{r})\rho(\vec{r}')}{|\vec{r}-\vec{r}'|}=Ce^2\frac{N^2}{2\Lambda},$$

where $A=0.4279$ as in the text, and $B=\Sigma_{j=1}^{3}\alpha_j\beta_j=1.365$, and $C=\Sigma_{j=1}^{3}\Sigma_{i=1}^{3}\alpha_i\alpha_j\beta_i\beta_j/(\beta_i+\beta_j)=0.4523$.

Thus one obtains the total energy $E_{\rm tot}=E_k+E_{ne}+\mu E_{ee}$ as a function of Λ. Here we introduced a variational parameter μ. The screening parameter Λ can be determined from the minimum condition $\partial E_{\rm tot}/\partial\Lambda=0$ to be

$$\Lambda=\frac{2AN^{2/3}}{BZ-(\mu/2)CN}.$$

Substituting this expression into $E_{\rm tot}$, and minimizing $E_{\rm tot}$ with respect to N for neutral-atom condition, i.e., $\partial E_{\rm tot}/\partial N=0$ at $N=Z$, one gets $\mu=2B/(7C)$. Substituting this relation into Λ, we finally obtain the expression

$$\Lambda=0.6269N^{2/3}a_0/(Z-N/7).$$

Equation (29) in the text is the Fourier transform of $\rho(\vec{r})$.

Concluding this appendix, we make a comment on Eq. (29). If we set $N=Z$ in Eq. (29), the screening length for neutral atoms is given by $\Lambda=0.7314Z^{-1/3}a_0$, which is close to the Thomas-Fermi (TF) screening length $\Lambda_{\rm TF}=0.8853Z^{-1/3}a_0$, and the resultant charge density in the Fourier space $\rho(\vec{k})$ is also close to the corresponding TF values. For comparison, Brandt and Kitagawa (BK) obtained $\Lambda_{\rm BK}=0.56Z^{-1/3}a_0$ for neutral atoms, using the electron density $\rho(\vec{r})=N/(4\pi\Lambda^2 r)\exp(-r/\Lambda)$ [30]. Our three-exponential-term description is actually a refinement of the BK model. In fact, the form factors $\rho(\vec{k})$ obtained by us for neutral atoms [set $N=Z$ in Eq. (29)] are rather closer to those calculated from the Hartree-Fock (HF) wave functions than the BK values. The BK model overestimates the screening of the bound electrons, resulting in the ion charge, $Z-\rho(\vec{k})$, in the Fourier space smaller than that in the HF and in the present cases. This feature of the BL model leads to, as an example, the electronic stopping powers for heavy ions much smaller than the HF and the present model at low velocities.

[1] A. B. Wittkower and H. D. Betz, At. Data **5**, 113 (1973).
[2] Y. Baudinet-Robinet, Phys. Rev. A **26**, 62 (1982).
[3] W. N. Lennard and D. Phillips, Phys. Rev. Lett. **45**, 176 (1980); W. N. Lennard, T. E. Jackson, and D. Phillips, Phys. Rev. A **24**, 2809 (1981).
[4] K. Shima, Nucl. Instrum. Methods Phys. Res. B **10**, 45 (1985).
[5] Haruyama, Ph.D thesis, Kyoto University, 1984 (unpublished).
[6] T. Kaneko and Y. H. Ohtsuki, Phys. Status Solidi B **111**, 491 (1982).
[7] H. D. Betz, Rev. Mod. Phys. **44**, 465 (1972); *Method of Experimental Physics* (Academic, New York 1980), Vol. 17, p. 73.
[8] K. Shima, T. Mikumo, and H. Tawara, At. Data Nucl. Data Tables **34**, 357 (1986).
[9] N. Bohr, K. Dan. Vidensk. Selsk. Mat. Fys. Medd. **18**, 8 (1948).
[10] H. D. Betz, Phys. Lett. **22**, 643 (1966).
[11] I. S. Dmitriev and V. S. Nikolaev, Zh. Eksp. Teor. Fiz. **47**, 615 (1964) [Sov. Phys. JETP **20**, 409 (1965)].
[12] M. Meron and B. Rosner, Phys. Rev. A **30**, 132 (1984).
[13] P. Attal, S. Della-Negra, D. Gardes, J. D. Larson, Y. Le. Beyec, R. Vienet-Legue, and B. Waast, Nucl. Instrum. Methods Phys. Res. A **328**, 293 (1993).
[14] B. Farizon, M. Farizon, M. J. Gaillard, E. Gerlic, and S. Ouaskit, Nucl. Instrum. Methods Phys. Res. B **88**, 86 (1994).
[15] A. Itoh, H. Tsuchida, T. Majima, and N. Imanishi, Phys. Rev. A **59**, 4428 (1999); A. Itoh, H. Tsuchida, T. Majima, S. Anada, Y. Yogo, and N. Imanishi, *ibid.* **61**, 012702 (2000); H. Tsuchida, A. Itoh, K. Miyabe, Y. Bitoh, and N. Imanishi, J. Phys. B **32**, 5289 (1999).
[16] T. LeBrun, H. G. Berry, S. Cheng, R. W. Dunfort, H. Esbensen, D. S. Gemmell, and E. P. Kanter, Phys. Rev. Lett. **72**, 3965 (1994).
[17] A. Faibis, G. Goldring, M. Hass, R. Kaim, I. Plesser, and Z. Vager, Nucl. Instrum. Methods **194**, 299 (1982).
[18] M. Vicanik, I. Abril, N. R. Arista, and A. Gras-Marti, Phys. Rev. A **46**, 5745 (1992).
[19] T. Kaneko, Nucl. Instrum. Methods Phys. Res. B **88**, 86 (1994).
[20] A. Brunelle, S. Della-Negra, J. Depauw, D. Jacquet, Y. Le. Beyec, M. Pautrat, and Ch. Schoppmann, Nucl. Instrum. Methods Phys. Res. B **125**, 207 (1997).
[21] T. Kaneko, Nucl. Instrum. Methods Phys. Res. B **153**, 15 (1999).
[22] E. Ray, R. Kirsch, H. H. Mikkelsen, J. C. Poizat, and J. Remillieux, Nucl. Instrum. Methods Phys. Res. B **69**, 133 (1992).
[23] K. Wohrer, M. Chabot, J. P. Rozet, D. Gardes, D. Vernhet, D. Jacquet, S. Della Negra, A. Brunelle, M. Nectoux, M. Pautrat, Y. Le. Beyec, P. Attal, and G. Maynard, J. Phys. B **29**, L755 (1996); M. Chabot, K. Wohrer, J. P. Rozet, D. Gardes, D. Vernhet, D. Jacquet, S. Della Negra, A. Brunelle, M. Nectoux, M. Pautrat, and Y. Le. Beyec, Phys. Scr. **T73**, 282 (1997).
[24] A. Brunelle, S. Della-Negra, J. Depauw, D. Jacquet, Y. Le. Beyec, and M. Pautrat, Phys. Rev. A **59**, 4456 (1999).

[25] T. Kaneko, Proc. Phys. Soc. Jpn. **55**, 87 (2000).
[26] Z. L. Miskovic, S. G. Davison, F. O. Goodman, W.-K. Liu, and Y.-N. Wang, Phys. Rev. A **61**, 062901 (2000).
[27] Z. L. Miskovic, W.-K. Liu, F. O. Goodman, and Y.-N. Wang, Phys. Rev. A **64**, 064901 (2001).
[28] Z. L. Miskovic, S. G. Davison, F. O. Goodman, W.-K. Liu, and Y.-N. Wang, Phys. Rev. A **63**, 022901 (2001).
[29] J. W. Hartman and T. A. Tombrello, Phys. Rev. A **62**, 043202 (2000).
[30] W. Brandt and M. Kitagawa, Phys. Rev. B **25**, 5631 (1982).
[31] T. Kaneko, Phys. Rev. A **51**, 535 (1995).
[32] W. Brandt, A. Ratkowski, and R. H. Ritchie, Phys. Rev. Lett. **33**, 1325 (1974).
[33] T. Kaneko, Phys. Rev. A **40**, 2188 (1989); Phys. Status Solidi B **156**, 49 (1989).
[34] T. Kaneko, At. Data Nucl. Data Tables **53**, 271 (1993).
[35] W. Weltner Jr. and R. J. VanZee, Chem. Rev. **89**, 1713 (1989).
[36] G. D. Carney and R. N. Porter, J. Chem. Phys. **65**, 3547 (1976).
[37] L. D. Landau and E. M. Lifshitz, *Quantum Mechanics*, 3rd ed. (Pergamon, Oxford, 1977).
[38] M. F. Steuer and R. H. Ritchie, Nucl. Instrum. Methods Phys. Res. B **40/41**, 372 (1989).
[39] K. Baudin, A. Brunelle, M. Chabot, S. Della-Negra, J. Depauw, D. Gardes, P. Hakansson, Y. Le. Beyec, A. Billebaud, M. Fallavier, J. Remillieux, J. C. Poizat, and J. P. Thomas, Nucl. Instrum. Methods Phys. Res. B **94**, 341 (1994).
[40] Z. Vager and D. S. Gemmell, Phys. Rev. Lett. **37**, 1352 (1976).